

Thalamic Neurons in the Pigeon Compute Distance-to-Collision of an Approaching Surface

Rui-Feng Liu Yu-Qiong Niu Shu-Rong Wang

Laboratory for Visual Information Processing, State Key Laboratory of Brain and Cognitive Sciences, Institute of Biophysics, Chinese Academy of Sciences, Beijing, China

Key Words

Distance-to-collision · Extracellular recording · Receptive field · Thalamus

Abstract

The thalamofugal and tectofugal pathways in birds are two parallel visual pathways to the telencephalon and might be comparable to the geniculocortical and colliculo-pulvinar-cortical pathways in mammals, respectively. It is known that some tectal neurons in the tectofugal pathway can signal the time-to-collision of an approaching object. Here we show by single cell recording in the pigeon that a population of visual neurons in the nucleus opticus principalis thalami (nOPT) in the thalamofugal pathway is able to detect the distance-to-collision of a large surface approaching towards the animal. These neurons began response firing when the surface reached a threshold distance to the viewing eye and thereafter their firing rates increased exponentially until collision occurred at distance = zero. The response onset distance is nearly constant for a wide range of stimulus velocities and is equal to the product of velocity of approaching stimulus and response onset time of a nOPT cell. Furthermore, onset distance of looming responses in nOPT cells is close to that causing cardioacceleration in the pigeon viewing the approaching surface. It appears that nOPT and tectal neurons are dichotomized functionally to a large extent for

detecting imminent dangers, and the pigeon's ability to compute the distance-to-collision of an approaching surface may benefit avoiding large obstacles during flight.

Copyright © 2008 S. Karger AG, Basel

Introduction

Humans and other animals move around in their environments full of a wide variety of objects and large surfaces and frequently interact with some objects or large surfaces during relative motion. Their ability to detect the optic variables of an object or large surface approaching towards the viewing eye is critical for avoiding dangerous collisions or achieving desirable interceptions. Single cell recording studies have indicated that some vi-

List of Abbreviations

ECG	Electrocardiogram
ERF	Excitatory receptive field
IRF	Inhibitory receptive field
nBOR	Nucleus of the basal optic root
nLM	Nucleus lentiformis mesencephali
nOPT	Nucleus opticus principalis thalami
OT	Optic tectum

KARGER

Fax +41 61 306 12 34
E-Mail karger@karger.ch
www.karger.com

© 2008 S. Karger AG, Basel
0006-8977/08/0721-0037\$24.50/0

Accessible online at:
www.karger.com/bbe

Shu-Rong Wang
Laboratory for Visual Information Processing
Institute of Biophysics, Chinese Academy of Sciences, 15 Datun Road
Beijing 100101 (P.R. China)
Tel. +86 10 6488 9858, Fax +86 10 6486 0713, E-Mail wangsr@sun5.ibp.ac.cn

sual neurons in several species are able to detect an object approaching towards the animal on a collision course [locust: Hatsopoulos et al., 1995; Rind and Simmons, 1999; Gabbiani et al., 2002; pigeon: Wang and Frost, 1992; Sun and Frost, 1998; Wu et al., 2005; Xiao et al., 2006; moth: Wicklein and Strausfeld, 2000; fish: Gallagher and Northmore, 2006; crab: Oliva et al., 2007]. Looming sensitive neurons in the locust visual system begin to respond when the angular retinal image size of an approaching object reaches a threshold value [Hatsopoulos et al., 1995; Rind and Simmons, 1999; Gabbiani et al., 2002], and those in the pigeon tectofugal pathway [optic tectum: Wu et al., 2005; nucleus rotundus: Sun and Frost, 1998; telencephalic entopallium: Xiao et al., 2006] are able to compute the time-to-collision and other optic variables of an approaching object. All these studies are devoted to the detection of an approaching object and assume that the object is not large and its motion velocity is constant [Rind and Simmons, 1999]. However, our knowledge is lacking about whether some visual neurons would respond to a large wall-like surface approaching towards the animal and, if so, what optic variables they would detect for signaling imminent collision with the surface.

The thalamofugal and tectofugal pathways in birds are two parallel visual pathways to the telencephalon, which might be comparable to the geniculocortical and colliculo-pulvinar-cortical pathways in mammals, respectively [Karten, 1969; Shimizu and Bowers, 1999; Krützfeldt & Wild, 2005; see fig. 1 in Yang et al., 2008]. The tectofugal pathway seems to process visual information in the whole field of view, whereas the thalamofugal pathway seems to be mainly involved in analysis of visual information in the lateral visual field [Remy and Güntürkün, 1991; Miceli et al., 2006]. Furthermore, neurons in the nucleus opticus principalis thalami (nOPT, a.k.a. nucleus geniculatus lateralis pars dorsalis) of the thalamofugal pathway and the optic tectum (OT) of the tectofugal pathway are different in their preferences for the direction and velocity of stimulus motion, and the excitatory receptive field (ERF) in nOPT cells is quite larger in size than that in tectal cells, showing that nOPT and OT cells would process different visual information [Yang et al., 2005]. In addition, nOPT receives afferents from the pretectal nucleus lentiformis mesencephali (nLM) and the nucleus of the basal optic root (nBOR) of the accessory optic system [Wild, 1989; Wylie et al., 1998; Cao et al., 2006]. The nucleus rotundus, a thalamic component of the tectofugal pathway, also receives input from nBOR [Wang et al., 2000; Diekamp et al., 2001], and some of its cells respond to an approaching object [Wang and

Frost, 1992; Sun and Frost, 1998]. Both nLM and nBOR are involved in generating optokinetic nystagmus induced by motion of large field stimuli [e.g. Fite et al., 1979; Gioanni et al., 1983a, b] and their neurons are selective for the direction, velocity and acceleration of visual motion [Gioanni et al., 1983a, b; Frost et al., 1990; Wolf-Oberhollenzer and Kirschfeld, 1994; Fu et al., 1998; Zhang et al., 1999; Cao et al., 2004]. Because looming sensitive OT neurons in the tectofugal pathway respond to an object but not to a large background approaching towards the animal [Wu et al., 2005], it is likely that looming sensitive nOPT neurons (if any) in the thalamofugal pathway may be able to detect an approaching surface.

In order to examine whether the pigeon nOPT cells would detect a large surface moving in depth, the present study was undertaken by using single cell recording, receptive field mapping and electrocardiogram (ECG) techniques. Our results provide electrophysiological evidence that a population of nOPT neurons in the pigeon can detect the distance-to-collision of a large surface approaching towards the viewing eye.

Materials and Methods

Preparations and Setup

The experiments were performed on 33 adult pigeons (*Columba livia*) of either sex, 320–500 g body weight, and complied with the regulations regarding the protection of animals established by the Council of the European Communities (Directive 86/609/EEC) and approved by the Institutional Animal Administration Committee. In physiological studies, each of 28 pigeons was anesthetized with an intramuscular injection of urethane (2 g/kg) and then placed on a foam couch in a stereotaxic apparatus. The scalp was incised and retracted, and the rostral tectum and caudal forebrain on the left side were exposed with a dental drill and surgical forceps. The dura mater overlying nOPT was excised for easy penetration of electrodes. The right eye was held open during recording and otherwise its lids were allowed to move freely and the left eye covered. During recording, eye movements were intermittently monitored by the experimenter and no observable eye movements were found in the pigeon under anesthesia [Gu et al., 2002; Niu et al., 2006]. A screen of 130° vertical × 140° horizontal was placed 40 cm away from the viewing eye. The horizontal axis of the visual field on the screen was rotated by 38° to match the pigeon's normal conditions [Erichsen et al., 1989; Fu et al., 1998; Niu et al., 2006; Li et al., 2007].

Five other pigeons were used to record ECG for examining whether the pigeon's heartbeat rate would be accelerated by the surface approaching towards the pigeon. Two steel electrodes (27-gauge syringe needles) were inserted into the bases of two wings of the alert pigeon with the one contralateral to the heart as reference [Wu et al., 2005]. ECG signals were magnified (1,000×) and filtered (DC to 300 Hz) with an amplifier (DAM 60, World Precision Instruments, USA) and fed into an oscilloscope (54622 A,

Agilent Technologies, USA) for display and stored in a computer (X900PI4, Asus, China) for off-line analysis. Heartbeats were accumulated in a time bin of 1 s and averaged in 5 repeats and then multiplied by 60 (beats/min). The data were fitted by a Gaussian function with the software SigmaPlot (Version 9.0, Systat Software Inc., USA). Cardioacceleration onset time was determined by an intersection of heart rate under control condition with the fitted curve to heart rate obtained under experimental condition [Wu et al., 2005].

Visual Stimuli

Three types of visual stimuli were generated by a computer with graphics (GeForce 7950 GT, Nvidia Corp., USA) and rear-projected onto the screen by a projector with refresh rate of up to 200 Hz (XG-C58X, Sharp Corp., Japan): (1) A whole-field pattern consisted of black random-dots with densities of $6\text{--}12 \times 10^3$ dots/m² and all the dots were moved as a whole stimulus. It simulated a wall-like surface and was moved in depth from simulated distance of 15 m at constant velocities of 1–7 m/s towards the viewing eye until it collided with the eye at distance = zero. In some cases, it was also used for comparing the responses of looming sensitive nOPT neurons to translational motion on the screen with those to in-depth motion towards the eye. (2) A soccer ball pattern (10–80 cm in diameter) with alternating black and white panels of equal areas, which was used to test whether surface-looming sensitive nOPT cells would also respond to the object approaching towards the animal [Sun and Frost, 1998; Wu et al., 2005; Xiao et al., 2006]. (3) A black square of 6° (visual angle) that was moved at 30–50°/s randomly along a series of parallel paths covering the whole screen for mapping the receptive field of a nOPT cell [Yang et al., 2005; Cao et al., 2006]. The ERF and inhibitory receptive field (IRF) of a spontaneously active cell were encompassed by the equal-rate line of 20% higher or lower than the spontaneous rate with the software Micrografx Picture Publisher (7a, Micrografx Inc., USA) [Cao et al., 2006]. The size of ERF and IRF was measured with the software Image-Pro Plus (Version 4.5.0.19, Media Cybernetics Inc.) [Li et al., 2007]. For a nOPT cell without spontaneous activity, its central ERF was plotted as above whereas its peripheral IRF (if any) was determined by gradually lengthening the square into a bar in the direction perpendicular to that of motion until the firing rate evoked by motion of the bar within ERF was reduced to a minimum [Wang et al., 2000; Yang et al., 2005]. In some experiments, differential contributions of ERF and IRF to looming responses were examined by stimulating either ERF or IRF alone through a restricted window [Fu et al., 1998].

The luminance of black and white in the visual stimuli was 0.1 and 6.6 cd/m², respectively. The stimulus first stayed on the screen for 3 s to collect spontaneous spikes as control and was then moved to examine looming responses in a thalamic cell, with an interval of 10 s between trials to allow the cell to recover from any motion adaptation.

Electrodes and Recording Sites

A micropipette (~2 μm tip diameter) filled with 2 M sodium acetate and 2% pontamine skyblue (Sigma Chemical Co., USA) was used for single cell recording and marking recording sites [Cao et al., 2004; Niu et al., 2006; Li et al., 2007]. The electrode was stereotaxically inserted into nOPT (A6.2–7.7, L2.5–4.0, H6.0–8.0) according to the pigeon's brain atlas [Karten and Hodos, 1967]. Neuronal spikes were magnified (1,000×) and filtered

(100–3,000 Hz) with the amplifier, displayed on the oscilloscope and fed into the computer for off-line analysis with the software CoolEdit (version 2.0, Syntrillium Software Corp., USA) and SigmaPlot (Version 9.0, Systat Software Inc., USA). Firing rates were accumulated and averaged in 3–10 repeats. Some recording sites were marked with pontamine skyblue (2%) deposited by negative current pulses of 10–20 (A in intensity and 0.5 s in duration at 1 Hz for 10–15 min [Cao et al., 2004; Niu et al., 2006; Yang et al., 2008].

At the end of experiments, each pigeon was euthanized by anesthesia overdose via an intraperitoneal injection of urethane (4 g/kg). For the pigeon with a recording site mark, the brain was removed from the skull and histologically processed for subsequent microscopic observation of the marked site.

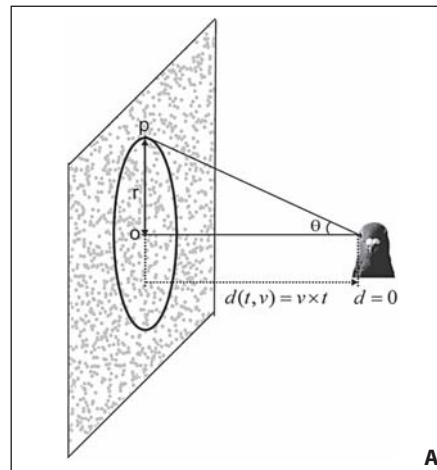
Results

Visual Responses of Thalamic Neurons to Motion in Depth

The experimental set-up is sketched in figure 1A showing that the pigeon viewed a textured surface on the screen and the surface was moved at a velocity v in depth and would collide with the animal at distance $d = 0$. Under such circumstances, 126 nOPT cells were examined in 28 pigeons for visual responses to the approaching surface. Among them, 35 cells (27.8%) responded to the surface with a characteristic firing pattern and 91 others (72.2%) did not respond this way and thus were omitted from further analysis. Each of the 35 cells did not respond until the surface reached a threshold distance to the eye, and then its firing rate increased exponentially until collision at distance = zero (fig. 2A–C). The spike rate before the threshold distance was not different from the spontaneous rate (paired t test, $t = 1.834$, $p = 0.076$, $n = 35$), and spike rates before and after the threshold distance were significantly different (paired t test, $t = 16.831$, $p < 0.001$, $n = 35$). The response histograms of an example nOPT cell to the approaching surface are graphed in figure 2A–C and fitted with an exponential function

$$f(d) = f_0 + C(v) \times \exp(Md)$$

where $f(d)$ is the instantaneous firing rate at distance d ; f_0 , $C(v)$ and M are constants related to the spontaneous rate, velocity preference and response onset distance of a given cell, respectively. The histograms seemed similar to those of tau cells signaling the time-to-collision [Sun and Frost, 1998; Wu et al., 2005; Xiao et al., 2006] because both looming sensitive cells enhance firing rate exponentially after a threshold time (tau cell) or distance (nOPT cell) is crossed. Histograms in figure 2A–C were fitted exponentially, and response onset distance was determined by an



According to the geometrical relationship
 $r(t) = vt \tan \theta$
 The ERF area at moment t is
 $S(t) = \pi [r(t)]^2$, and then $S(t) = \pi (vt \tan \theta)^2$
 The number of dots in the area
 $\varphi(t) = \rho \pi \tan^2 \theta v^2 t^2$
 Because the luminous flux received by the ERF is directly proportional to the number of dots, thus
 $\Phi(t) = K\varphi(t) = K\rho \pi \tan^2 \theta v^2 t^2$ (1)
 Both sides are differentiated with time
 $\Phi'(t) = 2K\rho \pi \tan^2 \theta v^2 t$ (2)
 Dividing equation (1) by equation (2) obtains
 $\frac{\Phi(t)}{\Phi'(t)} = \frac{t}{2}$
 Then $d(t, v) = v \times t$ becomes
 $d(t, v) = v \times \frac{2\Phi(t)}{\Phi'(t)}$

Fig. 1. Experimental set-up and mathematical functions of physical parameters defined in the present study. **A** A textured wall-like surface consisting of black random dots ($6\text{--}12 \times 10^3$ dots/m²) covered the whole screen (130° vertical \times 140° horizontal) that was placed tangential to and 40 cm away from the pigeon's viewing eye. It was moved at constant velocities $v = 1\text{--}7$ m/s from simulated distance of 15 m towards the pigeon. The radius $r(t)$ of ERF (circle) of a nOPT neuron subtended visual angle θ at the eye. The

approaching surface would collide with the animal when it reached distance $d(v, t) = 0$. **B** According to the geometrical relationship between physical parameters shown in A, the distance $d(t, v)$ of an approaching surface to the viewing eye could be computed by multiplication of the approaching velocity and the time remaining before collision. In the formulae, K is a coefficient and ρ is the density of random dots.

intersection of the fitted curve with a horizontal line defined by the spontaneous rate plus one standard deviation, indicating that this cell started response firing when the surface reached 6.23–6.32 m with an average of 6.29 ± 0.05 m to the viewing eye. Similar results were obtained for each of the 35 cells examined for 5 velocities and the data were linearly fitted with a slope of 0.07 and intercept of 5.91 m (fig. 2D). Two-way ANOVA analysis indicates that response onset distance of these cells was identical for all 5 velocities ($F_{4, 136} = 1.803$, $p = 0.132$) and averaged to be 6.10 ± 0.34 m. Figure 2E shows that response onset time of these cells was almost inversely proportional to velocity of the approaching surface as described by a polynomial function $y = y_0 + a/x$, because y_0 value was negligible (0.01) and thus constant $a = 6.08 \text{ m} \approx x$ (approaching velocity) \times y (response onset time) = response onset distance. Furthermore, distribution of the number of cells against response onset distance was graphed in figure 2F, which was fitted with a Lorentzian function peaked at response onset distance = 6.07 m. All this clearly indicates that response onset distance of these cells is ~ 6 m to the viewing eye and nearly equal to the product of approaching velocity and response onset time. It is noteworthy that this response onset distance did not depend on the densities of dots in the approaching surface. Two-way ANOVA analysis shows that the onset distances

of visual responses in 6 nOPT cells to approaching surfaces with different dot densities ($6, 8, 10, 12 \times 10^3$ dots/m²) were not different ($F_{3, 15} = 1.717$, $p = 0.206$).

To further provide evidence that nOPT cells are able to detect the distance-to-collision, we carried out so-called 'stopover experiments', in which the surface stopped moving somewhere beyond the response onset distance for a while and then resumed moving towards the animal. Figure 3 shows dependence of firing activity in an example nOPT cell on distance of the surface to the eye. The cell was not active during surface approach (3 m/s) until its threshold distance was reached. After the threshold distance was crossed, its firing increased exponentially but paused instantly when the surface stopped moving; the firing resumed as soon as the surface restarted moving after a stopover 15 s and kept increasing exponentially until collision occurred (fig. 3A, B, arrows). The response pattern combining both stages A and B (fig. 3C) seems similar to that evoked by non-stop motion (fig. 3D). This similarity was also demonstrated by the response histograms and their raster displays (5 repeats) (fig. 3E–H). Statistical analysis indicates that response of this cell to two-stage motion was not different from that to non-stop motion with respect to the response onset distance (6.78 vs. 6.96 m), peak rate (paired t test, $t = 0.272$, $p = 0.799$, $n = 5$) and mean rate (paired t test, $t =$

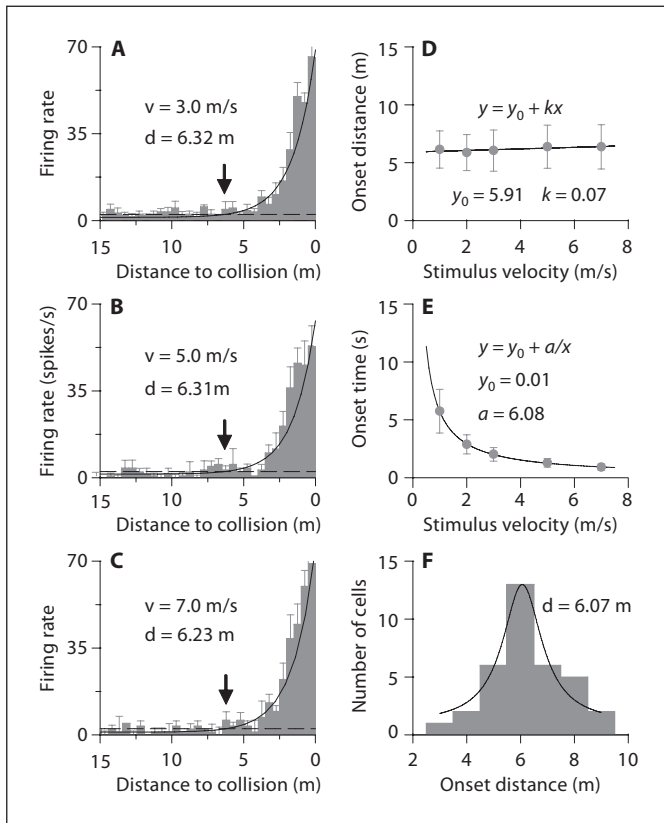


Fig. 2. Visual responses of nOPT cells depend on stimulus distance to the eye. A cell started firing when the surface approaching at velocities v reached threshold distance d and thereafter its firing rate increased exponentially until collision at $d = 0$ (A–C). Dashed lines represent the spontaneous rate plus SD and their intersections with the fitted curves determine response onset distance (arrows). Ten repeats, distance bin = 50 cm, error bar = SEM. Statistical data from 35 cells examined for 5 velocities are plotted in D–F. Data points (each for 35 cells) in D are linearly fitted. Relation of response onset time to approaching velocity is described by a polynomial function (E). Error bar = SD. Distribution of 35 cells against response onset distance is fitted with a Lorentzian function peaked at $d = 6.07$ m (F).

1.753, $p = 0.155$, $n = 5$). Four cells examined this way all demonstrated a similar pattern of visual responses to two-stage motion. Their responses to two-stage motion were not different from those to non-stop motion in terms of their response onset distance (paired t test, $t = 0.186$, $p = 0.865$, $n = 4$), peak rate (paired t test, $t = 0.532$, $p = 0.632$, $n = 4$) and mean rate (paired t test, $t = 1.830$, $p = 0.165$, $n = 4$). Three-way ANOVA analysis also indicates that responses evoked in these cells by two-stage motion and non-stop motion were not different ($F_{1,6} = 2.639$, $p = 0.155$, $n = 24$).

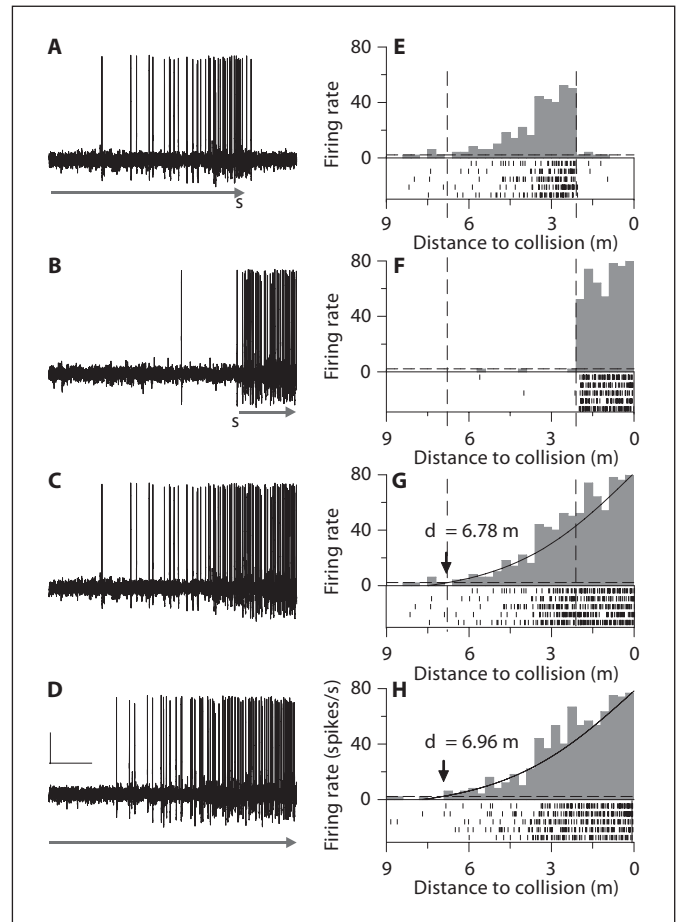


Fig. 3. Stopover experiments showing dependence of nOPT responses on distance of an approaching surface. Recording traces show that a cell started firing when the surface moving at 3 m/s reached threshold distance and then paused when the surface stopped moving (A, arrow s). Firing activity in the cell resumed instantly as the surface moved again (B, arrow s) and enhanced exponentially until collision. The total response (C) combining both stages A and B is identical to that to non-stop motion (D, arrow). Scales: 20 (V, 1.5 m. Histograms E–H (distance bin = 30 cm, 5 repeats) correspond to traces A–D with raster displays beneath, respectively. Horizontal dashed lines represent the spontaneous rate plus SD and their intersections with the fitted curves (G, H) determine response onset distance (d) and vertical ones delimit two stages of responses.

Differences between Thalamic Responses to In-Depth and Translational Motion

To exclude the possibility that visual responses of looming sensitive nOPT cells might be related to translation motion of the surface on the screen plane, we computer-mapped receptive fields of 20 out of 35 nOPT cells and compared their responses to the surface moving in

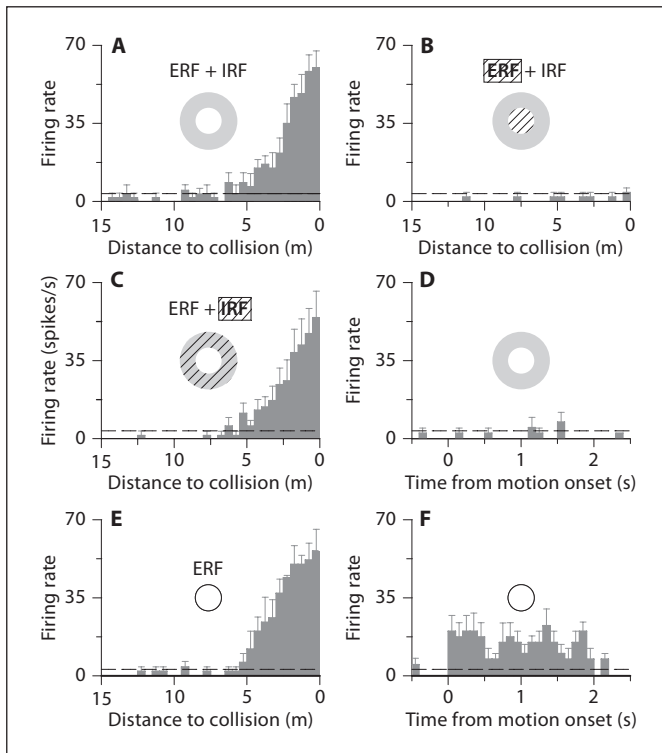


Fig. 4. Comparison is made between visual responses of two nOPT cells to in-depth motion and translational motion on the screen. Cell **A–D** with ERF-IRF responded to the approaching surface in ERF (**A, C**) but not in IRF (**B**). It did not show responses to translational motion due to balanced responses from both ERF and IRF (**D**). Cell EF possessing a single ERF responded to in-depth (**E**) and translational (**F**) motion with different firing patterns. Note that abscissa is scaled for distance-to-collision in **A–C** and **E** whereas it is scaled for time from motion onset in **D** and **F** because of translational motion. Open and grey circles represent ERF and IRF and their sheltered regions (hatched). Histograms are averaged in 5 repeats, error bar = SEM. Dashed lines represent the spontaneous rate plus SD. Distance bin = 50 cm and time bin = 100 ms.

depth and on the screen plane. According to receptive field organization, they were divided into two groups: group I contained 8 cells (40%) having concentric ERF-IRF and group II included 12 cells (60%) possessing a single ERF alone. The ERF was round or elliptic in shape and IRF was large and would extend beyond the screen in some cases. The size of ERF in group I cells was $29.8 \pm 13.8^\circ$ and that for group II cells was $33.8 \pm 15.2^\circ$. The ERF size was not different between the two groups (two-sample t test, $t = 0.599$, $p = 0.557$, $n_1 = 8$, $n_2 = 12$). Although all these cells responded to the approaching surface with a similar firing pattern that could be fitted by an expo-

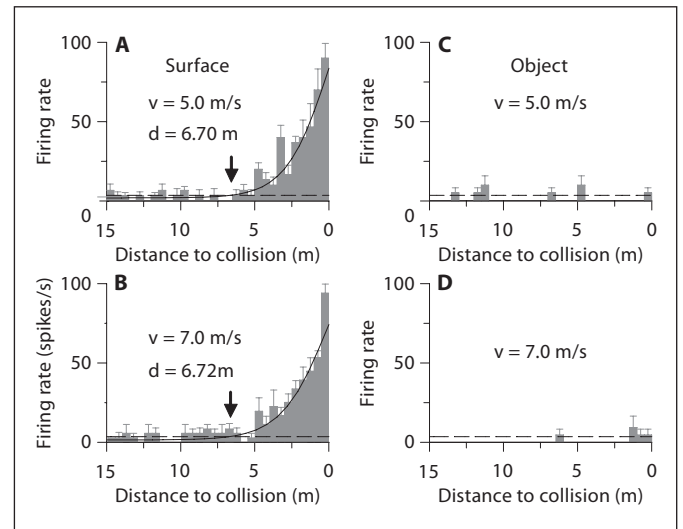


Fig. 5. Differential responses of a nOPT cell to a wall-like surface and soccer ball-like object approaching towards the pigeon. This cell had concentric ERF-IRF and responded to the surface with a characteristic firing pattern (**A, B**) but did not respond to the object (**C, D**). Either of stimuli was moved at velocities of 5–7 m/s. Response histograms are exponentially fitted and intersections of the fitted curves with the spontaneous rate plus SD (dashed lines) determine response onset distances (d , arrows). Five repeats, distance bin = 50 cm.

ponential function as stated above (fig. 4A, E), they responded differently to motion in depth and on the screen depending on receptive field organization. Group I cells did not respond to translational motion on the screen because excitatory responses from ERF were balanced by inhibitory responses from IRF (fig. 4D). However, IRF could not elicit any inhibitory responses to motion in depth so that it did not affect looming responses (fig. 4B, C). On the other hand, group II cells usually responded to translational motion of the surface such that visual responses persisted during the course of stimulus motion (fig. 4F). It appears that motion in depth evoked in nOPT cells a characteristic firing pattern different from that evoked by translational motion, and IRF would play a role only when the stimulus was moved on the screen plane.

Furthermore, 21 out of the 35 nOPT cells were also examined for visual responses to an object approaching towards the viewing eye. Among them, 10 cells (47.6%) produced no or little sporadic firing to the object (fig. 5) and 11 others (52.4%) responded to the object similarly to looming sensitive cells in the tectofugal pathway. They were classified into tau (1), eta (4) and rho (6) cells accord-

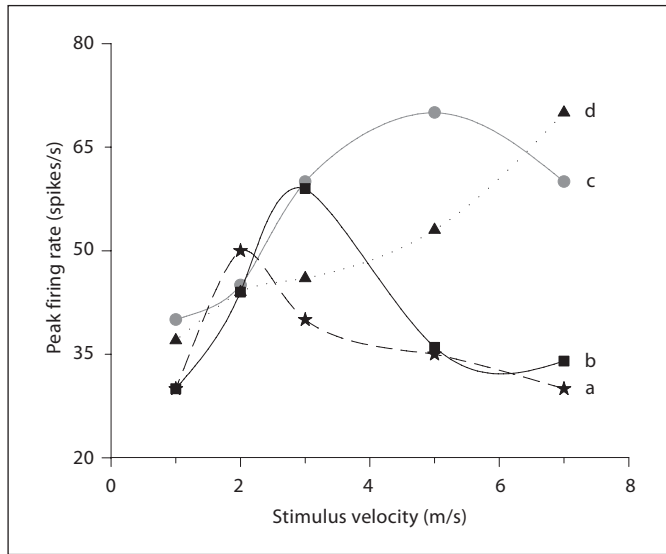


Fig. 6. Velocity-tuning curves of 4 looming sensitive nOPT neurons. Their responses to the surface (1×10^4 dots/m²) approaching towards the viewing eye were examined at velocities of 1–7 m/s and the data are fitted with B-spline interpolation. By using arbitrary criteria, cell a preferred low velocity (<3 m/s), cells b and c preferred immediate velocity (3–6 m/s), and cell d preferred high velocity (>6 m/s). Peak firing rate is averaged in 3 repeats.

ing to the criteria used by previous studies [Sun and Frost, 1998; Wu et al., 2005].

Because our statistical data show that response onset distance of a nOPT cell is equal to the product of approaching velocity of the surface and response onset time of the cell, we further explored whether nOPT cells would be able to detect the response onset time and the approaching velocity. Mathematical consideration in figure 1B indicates that distance $d(t, v)$ of the surface approaching at velocity v to the viewing eye could be calculated by the following formula:

$$d(t, v) = v \times \frac{2\Phi(t)}{\Phi'(t)}$$

where $\Phi(t)$ and $\Phi'(t)$ are the luminous flux (rate of flow of dots in this case) flowing through the ERF of a thalamic cell at the moment t and its rate of change over time, respectively. For example, when a surface (12×10^3 dots/m²) was 10, 5 and 0.4 m distant from the eye, the cell's ERF (e.g. 30°) contained 3×10^5 , 7×10^4 and 4×10^2 dots, respectively. It appears that the cell could calculate the ratio $\Phi(t)/\Phi'(t)$, i.e. response onset time, similar to computation of the time-to-collision by tau cells in the pigeon tectofugal pathway [Sun and Frost, 1998; Wu et

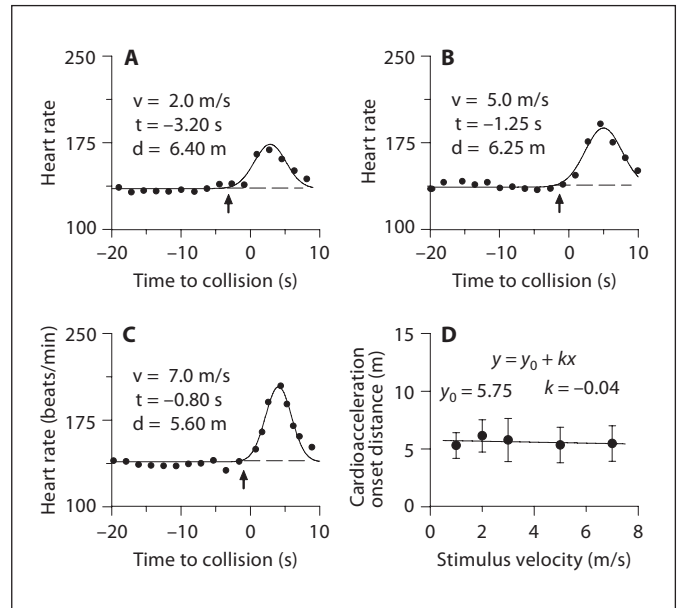


Fig. 7. Heartbeat rate in the pigeon is accelerated by the approaching surface. Cardioacceleration onset time (arrows) is determined by intersection of a mean heart rate under control condition (dashed lines) with Gaussian fitted curves to experimental data, showing that cardioacceleration onset time is delayed from 3.20 to 0.80 s before the time-to-collision and heart rate accelerated from 164 to 204 beats/min as velocities are increased from 2.0 to 7.0 m/s, respectively. Negative values in abscissa represent the time before collision at zero and three repeats are averaged (A–C). Data collected from 5 pigeons for 5 velocities are linearly fitted (D). Error bar = SD.

al., 2005; Xiao et al., 2006]. On the other hand, nOPT cells are selective not only for the velocity of translational motion on the screen [Yang et al., 2005] but also for that of motion in depth as shown by velocity-tuning curves of 4 typical cells (fig. 6). These tuning curves were measured with the surface approaching at 1–7 m/s and fitted by B-spline interpolation. By using arbitrary criteria to classify preferences for low (<3 m/s), immediate (3–6 m/s) and high (>6 m/s) velocity, 7 among the 35 cells (20%) preferred low velocity, 16 cells (45.7%) immediate velocity and 12 others (34.3%) high velocity. It seems that nOPT cells may be also able to encode the velocity of motion in depth.

Cardioacceleration Evoked by an Approaching Surface

The textured surface approaching towards the pigeon not only evoked looming responses in nOPT cells but also accelerated the pigeon's heartbeat rate. Figure 7A–C shows that cardioacceleration onset time was earlier

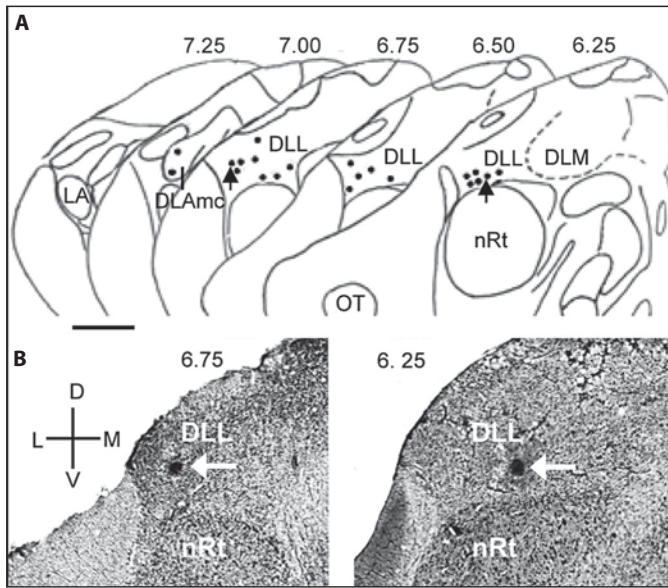


Fig. 8. Photomicrographs and drawings of the pigeon's brain cross-sections show distribution of 21 recording sites (dots). Two recording sites in **A** (arrows) correspond to dye marks in sections **B** (white arrows). These sites are localized in nOPT divisions including the nucleus dorsolateralis anterior thalami pars lateralis (DLL) and pars magnocellularis (DLAmc) but not in the nucleus lateralis anterior thalami (LA). Other abbreviations: DLM = Nucleus dorsolateralis anterior thalami pars medialis; nRt = Nucleus rotundus; OT = Optic tectum. Numerals represent the anterior-posterior levels 7.25–6.25 [Karten and Hodos, 1967]. D, L, V and M represent dorsal, lateral, ventral and medial, respectively. Scale bar = 1 mm in **A** and 0.5 mm in **B**.

(3.20 s in A) for a low velocity (2.0 m/s) than that (0.80 s in C) for a high velocity (7.0 m/s), but the peak heart rate was smaller for the low velocity than that for the high velocity (164 vs. 204 beats/min). However, cardioacceleration onset distances measured at these velocities were quite similar (d values in fig. 7A–C). Statistical analysis for two extreme velocities (1 and 7 m/s) examined in 5 pigeons indicates that cardioacceleration onset time for 1 m/s (5.30 ± 1.12 s) was much earlier than that for 7 m/s (0.78 ± 0.22 s) and thus cardioacceleration onset time differed between the tested velocities (paired t test, $t = 9.350$, $p < 0.001$, $n = 5$). On the other hand, the peak heart rate for 1 m/s was lower (174.50 ± 13.09 beats/min) than that for 7 m/s (218.22 ± 40.90 beats/s) and these two heart rates were different (paired t test, $t = 2.375$, $p = 0.038$, $n = 5$). Figure 7D shows that the data obtained from 5 pigeons for 5 velocities were fitted by a linear function $y = y_0 + kx$ with slope k being -0.04 and intercept 5.75 m. Because the k value was negligible, cardioacceleration

onset distance was nearly 5.75 m. Two-way ANOVA analysis indicates that cardioacceleration onset distance in 5 pigeons was equal for all 5 velocities ($F_{4,16} = 0.781$, $p = 0.554$) and averaged to be 5.60 ± 0.35 m, which approximates the response onset distance of looming sensitive nOPT neurons (6.10 ± 0.34 m, $n = 35$). All this indicates that the approaching surface is a threatening stimulus for the pigeon and visual responses of surface-looming sensitive nOPT cells may be somehow related to changes in the pigeon's heartbeat rate.

Histological Confirmation of Recording Sites

The recording sites of 21 looming sensitive neurons were marked with dye and all localized within nOPT with an uneven distribution in its various subdivisions, including 19 in the nucleus dorsolateralis anterior thalami pars lateralis (DLL) and 2 in the nucleus dorsolateralis anterior thalami pars magnocellularis (DLAmc). None of these marks was found in the nucleus lateralis anterior thalami (LA) (fig. 8).

Discussion

Previous studies have indicated that looming sensitive neurons in the pigeon tectofugal pathway signal the time-to-collision of an object approaching towards the animal on a collision course [Wang and Frost, 1992; Sun and Frost, 1998; Wu et al., 2005; Xiao et al., 2006]. The present study is the first to provide physiological evidence that about 30% of nOPT cells examined in the pigeon are able to detect the distance-to-collision of a large surface approaching towards the animal; half of them also can compute the time-to-collision of an approaching object. It appears that visual cells in nOPT and OT in birds are dichotomized functionally to a large extent for signaling imminent dangers. The textured surface we used is different from the optic flow patterns used in previous studies on the monkey medial superior temporal area [Tanaka et al., 1989; Churchland and Lisberger, 2005; Gu et al., 2006] and on the cat lateral suprasylvian area [Li et al., 2000; Chen et al., 2004] because all the components of the surface are moved collectively as a whole stimulus in depth, whereas those of the optic flow patterns are moved individually in a translational or radial expansion way. Furthermore, visual responses of nOPT cells to the approaching surface are not evoked by lateral translation of the surface because they respond differently to in-depth motion and translational motion on the screen.

The present study shows that looming sensitive nOPT cells do not discharge response spikes until the approaching surface reaches a threshold distance to the viewing eye and thereafter the firing rate is increased exponentially to its peak when collision occurs. Though the firing pattern in nOPT cells seems similar to that of tau cells in the tectofugal pathway, the response onset time in nOPT cells is variable and inversely proportional to the velocity of an approaching surface, whereas the response onset time of tau cells is constant and independent of the velocity of an approaching object [Wang and Frost, 1992; Sun and Frost, 1998; Wu et al., 2005; Xiao et al., 2006]. However, the response onset distance of a nOPT cell is nearly constant for a wide range of velocities and equals the product of the response onset time of the cell and the velocity of an approaching surface. In addition, this response onset distance does not depend on dot densities in the approaching surface. Furthermore, nOPT cells stop response firing immediately after the surface stops moving beyond the threshold distance and then restart firing instantly when motion is resumed after stopover. Total responses to two-stage motion are identical to those to non-stop motion, indicating that firing activity in nOPT cells depends on the distance of the surface to the viewing eye.

It is interesting to note that the pigeon viewing an approaching surface begins accelerating its heartbeat rate when the surface reaches a threshold distance to the viewing eye. The finding that the threshold distance for visual responses parallels to cardioacceleration onset distance implies that the surface we used is a dangerous stimulus for the animal and that nOPT activity could affect heartbeat rates in some way [Gibbs et al., 1986].

Behavioral studies have indicated that animals are able to estimate object distance by using stereopsis, motion parallax [Sobel, 1990; Schuster et al., 2002; Olberg et al., 2005] or retinal image size information [Goodale et al., 1990; Ellard, 2004]. However, how nOPT cells would be able to compute the distance-to-collision of an approaching surface is unknown. It is possible that the pigeon could detect the distance in some way by using monocular cues because it is far-sighted in the monocular field [Catania, 1964; Bloch and Martinoya, 1982] and nOPT cells receive afferents from large retinal ganglion cells mainly corresponding to the lateral visual field [Remy and Güntürkün, 1991; Güntürkün and Hahmann, 1999; Miceli et al., 2006]. Previous studies on primates have indicated that there may be several cues for detecting depth information [Howard, 2003]. However, it is likely that nOPT cells may be able to detect the time-to-

collision and the velocity of an approaching surface, and then implement multiplication to determine the distance-to-collision. These cells can determine the time-to-collision of an approaching surface by using luminous flux $\Phi(t)$ divided by its change rate over time $\Phi'(t)$ in a similar way to operation implemented by tau cells in the tectofugal pathway [Sun and Frost, 1998; Wu et al., 2005; Xiao et al., 2006]. The finding that the response onset distance of nOPT cells does not depend on dot densities in the surface indicates that the time-to-collision is not determined by angular size of a dot or inter-dot distance in the surface. Although neural mechanisms underlying detection of approaching velocity by nOPT cells are still unknown, they may be related to nOPT selectivity for velocity and /or velocity-related information from optokinetic structures nBOR/nLM, which are highly selective for the velocity, acceleration and direction of stimulus motion [Gioanni et al., 1983a, b; Wolf-Oberhollenzer and Kirschfeld, 1994; Fu et al., 1998; Zhang et al., 1999, Cao et al., 2004; Niu et al., 2006].

Response onset distance of looming sensitive nOPT cells may provide a critical warning signal so that the pigeon would be able to know its distance to a large surface or flock of birds based on distance-related firing rates. In this regard, the pigeon may behave like the fruit fly, in which a large surface approaching in the monocular field may trigger avoidance responses whereas that approaching in the binocular field would initiate landing responses [Tammero and Dickinson, 2002]. Landing relevant neurons in the pigeon may be found in the ventral tectum, where most of visual neurons have receptive fields in the binocular field [Gu et al., 2000].

Acknowledgments

This work was supported by the National Natural Science Foundation of China (90208008) and by the Chinese Academy of Sciences (KSCX1-YW-R-32).

References

- Bloch S, Martinoya C (1982) Comparing frontal and lateral viewing in the pigeon. I. Tachistoscopic visual acuity as a function of distance. *Behav Brain Res* 5:231–244.
- Cao P, Gu Y, Wang SR (2004) Visual neurons in the pigeon brain encode the acceleration of stimulus motion. *J Neurosci* 24:7690–7698.
- Cao P, Yang Y, Wang SR (2006) Differential modulation of thalamic neurons by optokinetic nuclei in the pigeon. *Brain Res* 1069:159–165.
- Catania AC (1964) On the visual acuity of the pigeon. *J Exp Anal Behav* 7:361–366.
- Chen H, Li B, Diao YC (2004) Response properties of neurons in cat dorsal lateral suprasylvian cortex to optic flow fields. *Neuroreport* 15:1019–1023.
- Churchland AK, Lisberger SG (2005) Discharge properties of MST neurons that project to the frontal pursuit area in macaque monkeys. *J Neurophysiol* 94:1084–1090.
- Diekamp B, Hellmann B, Troje NF, Wang SR, Güntürkün O (2001) Electrophysiological and anatomical evidence for a direct projection from the nucleus of the basal optic root to the nucleus rotundus in pigeons. *Neurosci Lett* 305:103–106.
- Ellard CG (2004) Visually guided locomotion in the gerbil: a comparison of open- and closed-loop control. *Behav Brain Res* 149:41–48.
- Ericksen JT, Hodos W, Evinger C, Bessette BB, Phillips SJ (1989) Head orientation in pigeon: postural, locomotor and visual determinants. *Brain Behav Evol* 33:268–278.
- Fite KV, Reiner A, Hunt SP (1979) Optokinetic nystagmus and the accessory optic system of pigeon and turtle. *Brain Behav Evol* 16:192–202.
- Frost BJ, Wylie DR, Wang YC (1990) The processing of object and self-motion in the tectofugal and accessory optic pathways of birds. *Vision Res* 30:1677–1688.
- Fu YX, Gao HF, Guo MW, Wang SR (1998) Receptive field properties of visual neurons in the avian nucleus lentiformis mesencephali. *Exp Brain Res* 118:279–285.
- Gabbiani F, Krapp HG, Koch C, Laurent G (2002) Multiplicative computation in a visual neuron sensitive to looming. *Nature* 420:320–324.
- Gallagher SP, Northmore DP (2006) Responses of the teleostean nucleus isthmi to looming objects and other moving stimuli. *Vis Neurosci* 23:209–219.
- Gibbs CM, Cohen DH, Broyles JL (1986) Modification of the discharge of lateral geniculate neurons during visual learning. *J Neurosci* 6:627–636.
- Gioanni H, Rey J, Villalobos J, Richard D, Dalbera A (1983a) Optokinetic nystagmus in the pigeon (*Columba livia*). II. Role of the pretectal nucleus of the accessory optic system (AOS). *Exp Brain Res* 50:237–247.
- Gioanni H, Villalobos J, Rey J, Dalbera A (1983b) Optokinetic nystagmus in the pigeon (*Columba livia*). III. Role of the nucleus ectomamillaris (nEM): interactions in the accessory optic system (AOS). *Exp Brain Res* 50:248–258.
- Goodale MA, Ellard CG, Booth L (1990) The role of image size and retinal motion in the computation of absolute distance by the Mongolian gerbil (*Meriones unguiculatus*). *Vision Res* 30:399–413.
- Gu Y, Wang Y, Wang SR (2000) Regional variation in receptive field properties of tectal neurons in pigeons. *Brain Behav Evol* 55:221–228.
- Gu Y, Wang Y, Wang SR (2002) Visual responses of neurons in the nucleus of the basal optic root to stationary stimuli in pigeons. *J Neurosci Res* 67:698–704.
- Gu Y, Watkins PV, Angelaki DE, DeAngelis GC (2006) Visual and nonvisual contributions to three-dimensional heading selectivity in the medial superior temporal area. *J Neurosci* 26:73–85.
- Güntürkün O, Hahmann U (1999) Functional subdivisions of the ascending visual pathways in the pigeon. *Behav Brain Res* 98:193–201.
- Hatsopoulos N, Gabbiani F, Laurent G (1995) Elementary computation of object approach by a wide-field visual neuron. *Science* 270:1000–1003.
- Howard IP (2003) Neurons that respond to more than one depth cue. *Trends Neurosci* 26:515–517.
- Karten HJ (1969) The organization of the avian telencephalon some speculations on the phylogeny of the amniote telencephalon. *Ann NY Acad Sci* 167:164–180.
- Karten HJ, Hodos W (1967) *A Stereotaxic Atlas of the Brain of the Pigeon (Columba livia)*. Baltimore MD: Johns Hopkins Press.
- Krützfeldt NO, Wild JM (2005) Definition and novel connections of the entopallium in the pigeon (*Columba livia*). *J Comp Neurol* 490:40–56.
- Li B, Li BW, Chen Y, Wang LH, Diao YC (2000) Response properties of PMLS and PLLS neurons to simulated optic flow patterns. *Eur J Neurosci* 12:1534–1544.
- Li DP, Xiao Q, Wang SR (2007) Feedforward construction of the receptive field and orientation selectivity of visual neurons in the pigeon. *Cereb Cortex* 17:885–893.
- Miceli D, Reperant J, Medina M, Volle M, Rio JP (2006) Distribution of ganglion cells in the pigeon retina labeled via retrograde transneuronal transport of the fluorescent dye rhodamine beta-isothiocyanate from the telencephalic visual Wulst. *Brain Res* 1098:94–105.
- Niu YQ, Xiao Q, Liu RF, Wu LQ, Wang SR (2006) Response characteristics of the pigeon's pretectal neurons to illusory contours and motion. *J Physiol (Lond)* 577:805–813.
- Olberg RM, Worthington AH, Fox JL, Bessette CE, Loosemore MP (2005) Prey size selection and distance estimation in foraging adult dragonflies. *J Comp Physiol A* 191:791–797.
- Oliva D, Medan V, Tomsic D (2007) Escape behavior and neuronal responses to looming stimuli in the crab *Chasmagnathus granulatus*. *J Exp Biol* 210:865–880.
- Remy M, Güntürkün O (1991) Retinal afferents to the tectum opticum and the nucleus opticus principalis thalami in the pigeon. *J Comp Neurol* 305:57–70.
- Rind FC, Simmons PJ (1999) Seeing what is coming: building collision-sensitive neurons. *Trends Neurosci* 22:215–220.
- Shimizu T, Bowers AN (1999) Visual circuits of the avian telencephalon: evolutionary implications. *Behav Brain Res* 98:183–191.
- Schuster S, Strauss R, Gotz KG (2002) Virtual-reality techniques resolve the visual cues used by fruit flies to evaluate object distances. *Curr Biol* 12:1591–1594.
- Sobel EC (1990) The locust's use of motion parallax to measure distance. *J Comp Physiol A* 167:579–588.
- Sun HJ, Frost BJ (1998) Computation of different optical variables of looming objects in pigeon nucleus rotundus neurons. *Nat Neurosci* 1:296–303.
- Tammero LF, Dickinson MH (2002) Collision-avoidance and landing responses are mediated by separate pathways in the fruit fly, *Drosophila melanogaster*. *J Exp Biol* 205:2785–2798.
- Tanaka K, Fukada Y, Saito HA (1989) Underlying mechanisms of the response specificity of expansion/contraction and rotation cells in the dorsal part of the medial superior temporal area of the macaque monkey. *J Neurophysiol* 62:642–656.
- Wang Y, Xiao J, Wang SR (2000) Excitatory and inhibitory receptive fields of tectal cells are differentially modified by magnocellular and parvocellular divisions of the pigeon nucleus isthmi. *J Comp Physiol A* 186:505–511.
- Wang Y, Gu Y, Wang SR (2000) Modulatory effects of the nucleus of the basal optic root on rotundal neurons in pigeons. *Brain Behav Evol* 56:287–292.
- Wang YC, Frost BJ (1992) 'Time to collision' is signaled by neurons in the nucleus rotundus of pigeon. *Nature* 356:236–238.
- Wickelmaier M, Strausfeld NJ (2000) Organization and significance of neurons that detect change of visual depth in the hawk moth *Manduca sexta*. *J Comp Neurol* 424:356–376.

- Wild JM (1989) Pretectal and tectal projections to the homologue of the dorsal lateral geniculate nucleus in the pigeon: an anterograde and retrograde tracing study with cholera toxin conjugated to horseradish peroxidase. *Brain Res* 479:130–137.
- Wolf-Oberhollenzer F, Kirschfeld K (1994) Motion sensitivity in the nucleus of the basal optic root of the pigeon. *J Neurophysiol* 71:1559–1573.
- Wu LQ, Niu YQ, Yang J, Wang SR (2005) Tectal neurons signal impending collision of looming objects in the pigeon. *Eur J Neurosci* 22:2325–2331.
- Wylie DR, Glover RG, Lau KL (1998) Projections from the accessory optic system and pretectum to the dorsolateral thalamus in the pigeon (*Columbia livia*): A study using both anterograde and retrograde tracers. *J Comp Neurol* 391:456–469.
- Xiao Q, Li DP, Wang SR (2006) Looming sensitive responses and receptive field organization of telencephalic neurons in the pigeon. *Brain Res Bull* 68:322–328.
- Yang J, Zhang C, Wang SR (2005) Comparisons of visual properties between tectal and thalamic neurons with overlapping receptive fields in the pigeon. *Brain Behav Evol* 65:33–39.
- Yang Y, Cao P, Yang Y, Wang SR (2008) Corollary discharge circuits for saccadic modulation of the pigeon visual system. *Nat Neurosci* 11:595–602.
- Zhang T, Fu YX, Hu J, Wang SR (1999) Receptive field characteristics of neurons in the nucleus of the basal optic root in pigeons. *Neuroscience* 91:33–40.